APR. 1999 VOL. 4 NO. 2
ISSN 1084-0699
CODEN: JHYEFF

JOURNAL OF HYDROLOGIC ENGINEERING

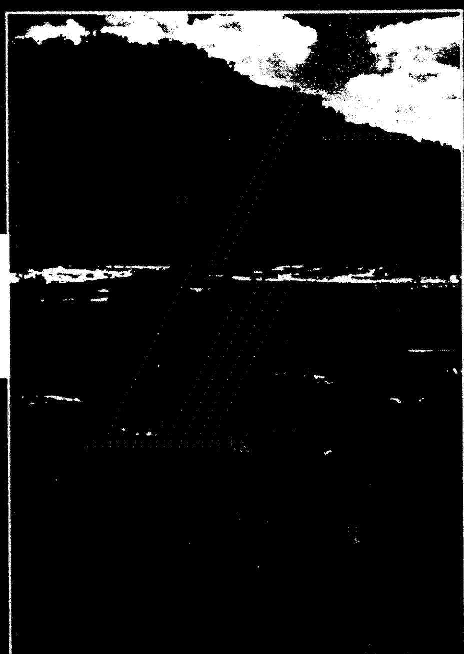

ASCE

American Society of Civil Engineers
Water Resources Engineering Division

TECHNICAL PAPERS

contents continued on back cover

Comparing Mean Areal Precipitation Estimates from NEXRAD and Rain Gauge Networks

By Dennis Johnson,[1] Michael Smith,[2] Victor Koren,[3] and Bryce Finnerty[4]

Abstract: Mean areal precipitation values (MAPX) derived from next generation weather radar (NEXRAD) stage III data are compared with mean areal precipitation (MAP) values derived from a precipitation gauge network. The gauge-derived MAPs are computed using Thiessen polygon weighting, whereas the radar-based MAPXs utilize the gridded stage III radar precipitation products that have been conditioned with gauge measurements and have been merged with overlapping radar fields. We compare over 4,000 pairs of MAPX and MAP estimates over a 3-year time period for each of eight basins in the southern plains region of the United States. Over the long term, mean areal estimates derived from NEXRAD generally are 5–10% below gauge-derived estimates. In the smallest basin, the long-term MAPX mean was greater than the MAP. For storm events, a slight tendency for NEXRAD to measure fewer yet more intense intervals of precipitation is identified. Comparison of hydrologic simulations using the two forcings indicates that significant differences in runoff volume can result. This work is aimed at providing insight into the use of a data product that is becoming increasingly available for public use. It also is aimed at investigating the use of radar data in hydrologic models that have been calibrated using gauge-based precipitation estimates.

INTRODUCTION

Overview of the National Weather Service River Forecast System (NWSRFS)

The National Weather Service (NWS) is in the unique position of being required by law to provide river forecasts for the entire United States. Currently, daily forecasts are issued at over 4,000 points. To accomplish this task, the NWS uses the NWSRFS, which contains over 500,000 lines of executable computer code. The NWSRFS is comprised of a number of procedures for end-to-end processing from data collection to forecast generation.

As seen in Fig. 1, the NWSRFS actually is a suite of three systems. In the calibration system, historical time series are created from streamflow and mean areal estimates of precipitation, temperature, and other data. Raw data for deriving these estimates are retrieved from the National Climatic Data Center (NCDC) archive. With the use of these historical time series, manual and automatic procedures are used to derive calibrated parameters for the hydrologic models used in the forecast operations. An important assumption is that the mean areal estimates derived from the historical gauge network are similar statistically to those derived from the operational gauge network. In the operational forecast system (OFS), real-time observed data are used with the calibrated hydrologic models to generate short-term hydrologic forecasts. Interactive adjustments to model parameters and states can be made during run time using the interactive forecast program. Longer term probabilistic forecasts within the ensemble streamflow prediction system are made using elements from both the calibration system and the OFS. Historical time series are used to generate an ensemble of streamflow forecasts with the models being initialized by the current soil moisture states maintained within the OFS. It is important to note that the same hydrologic models are used in all three systems. Therefore, the process of calibration is critical for both short-term and long-term river forecasting. Properly calibrated models are very important for ensemble streamflow prediction forecasts in that there is no provision for run-time adjustments to the model parameters and states.

Problem Description

Until recently, precipitation input for operational forecasting has been based solely on point rain gauge measurements that are converted into mean areal precipitation estimates. With the nationwide deployment of the Weather Surveillance Radar-1988 Doppler (WSR-88D) systems known as next-generation weather radar (NEXRAD), the NWS and others have the opportunity to use hourly 4-km precipitation estimates for hydrologic modeling (Hudlow 1988; Klazura and Imy 1993). Given these new precipitation products, the NWS is investigating semidistributed hydrologic modeling to improve its ability to simulate and predict river flows. One aspect of this investigation is to understand the differences between rain gauge-derived and radar-derived estimates of mean areal precipitation, because often both are used for operational forecasting in the same basin. Hereafter, we define the acronym MAP to refer to the mean areal estimates derived from a rain gauge network, whereas MAPX will refer to those defined using radar mesurements.

Other investigations indicate that differences between MAP and MAPX do exist. In an early study, Smith et al. (1975) noticed a general underestimation of daily mean areal rainfall derived by radar compared with that derived from a rain gauge network. Barge et al. (1979) compared rain gauge- and radar-derived mean areal rainfall estimates for a 6-day storm sequence. Clearly, they were able to identify causes for large differences in the two estimates. Collier et al. (1975) were able to show that the addition of rain gauges used in calibrating radar led to improved estimates of areal rainfall. For a 7-month period, Finnerty and Johnson (1997) compared MAP values derived from the NCDC gauge network with MAPX values for several basins near Tulsa, Okla. Their findings indicated that the mean areal precipitation estimates derived from NEXRAD are biased low compared with gauge-derived estimates. Borga et al. (1995) compared several radar-derived mean areal estimates with several gauge products. In streamflow simulations limited to one storm event, they investigated

---

[1]Asst. Prof., Michigan Tech. Univ., 312 Chemical Sci. Build., 1400 Townsend Dr., Houghton, MI 49931-1295. E-mail: dennisj@mtu.edu

[2]Res. Hydro., Nat. Weather Service, Hydrologic Res. Lab., W/OH-1, 1325 East West Hwy., Silver Spring, MD 20910. E-mail: mbs@skipper.nws.noaa.gov

[3]Res. Hydro., Nat. Weather Service, Hydrologic Res. Lab., W/OH-1, 1325 East West Hwy., Silver Spring, MD. E-mail: vkoren@skipper.nws.noaa.gov

[4]Engr., Dewberry and Davis, 8401 Arlington, VA 22031.

Note. Discussion open until September 1, 1999. To extend the closing date one month, a written request must be filed with the ASCE Manager of Journals. The manuscript for this paper was submitted for review and possible publication on September 18, 1997. This paper is part of the *Journal of Hydrologic Engineering*, Vol. 4, No. 2, April, 1999. ©ASCE, ISSN 1084-0699/99/0002-0117–0124/$8.00 + $.50 per page. Paper No. 16451.

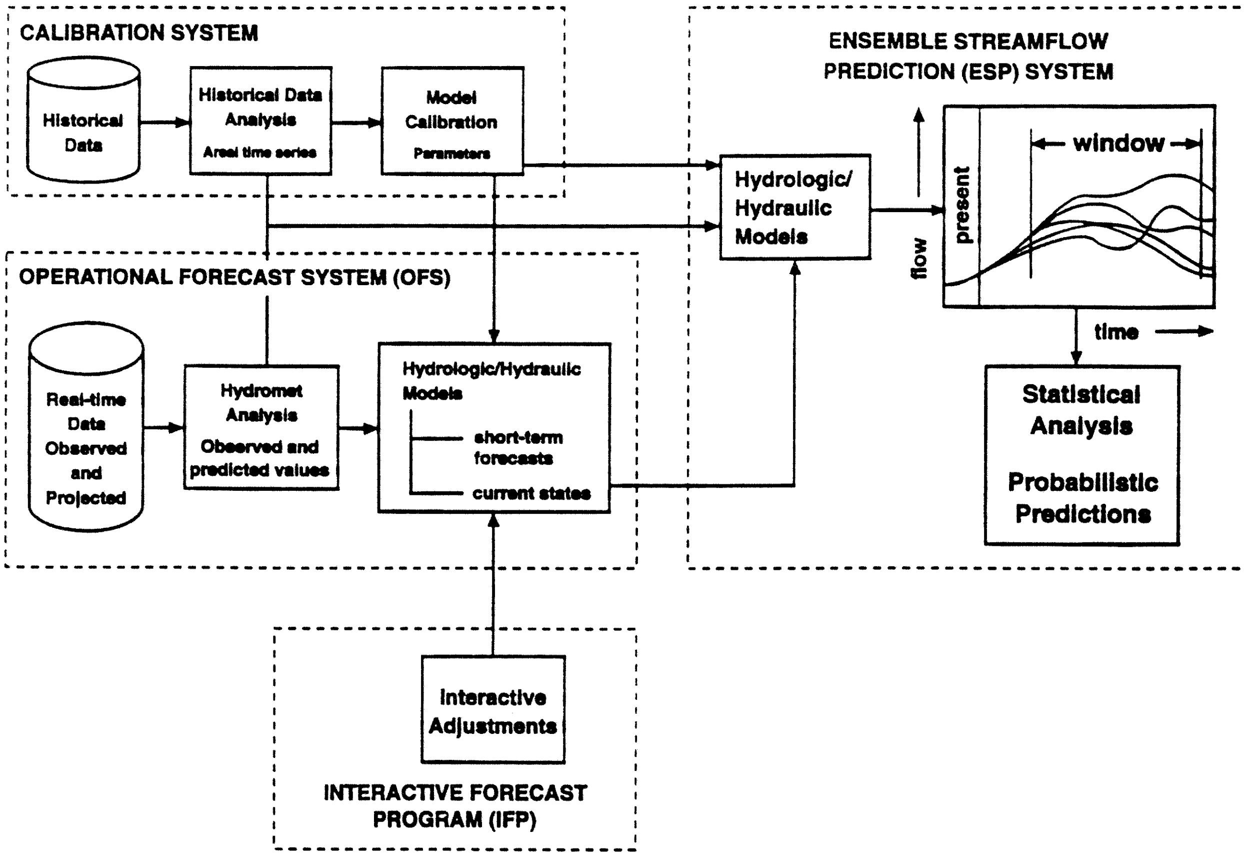

FIG. 1. Schematic Diagram of Major Components of NWSRFS

the hydrologic impacts of the differences in the mean areal products. Goodhew and Mylne (1992) compared daily mean areal estimates from rain gauge networks of various density to those based on data from a single radar. Their analysis spanned a 2-year period. Agreement between the two estimates was found to vary with distance from the radar, amount of gauge-recorded precipitation, radar calibration, and location under the radar umbrella. Finnerty et al. (1997) found that parameters for the Sacramento soil moisture accounting (SAC-SMA) model are linked strongly to the temporal and spatial scale of precipitation forcing, implying that hydrologic model parameters calibrated from rain gauge networks may not be suitable for use with the gridded NEXRAD data.

In light of these findings, it is important that the two estimates of precipitation forcing be understood. The following two objectives of this paper are identified: (1) To examine the statistical differences between radar-derived and gauge-derived estimates of mean areal precipitation; and (2) to investigate the potential impacts of these differences on streamflow simulations generated with a hydrologic model commonly used within the NWS. This initial study is not aimed at investigating the accuracy of the two mean areal precipitation products themselves or subsequently derived streamflow simulations, but rather to provide a comparison. Differences in these products undoubtedly will have implications on calibrated parameters, mean areal precipitation estimates, and climate and hydrologic modeling.

METHODOLOGY

Basins within the domain of the Arkansas-Red Basin River Forecast Center were chosen for these comparisons for several reasons. This area has the longest archive of radar data available and it has a relatively dense rain gauge network in comparison with some areas of the country. The density of the rain gauge network is in reference to the operational gauges and the network of gauges used in producing the stage III radar precipitation estimates. In addition, there are a number of unregulated headwater basins already being modeled by the Arkansas-Red Basin River Forecast Center. The basic framework of the methodology includes the following: (1) Obtain operational 6-h MAP estimates from the Tulsa River Forecast Center data archives for the period from 1993 to 1996; (2) for the same 1993–1996 period, obtain operationally derived 1-h MAPXs for the same basins and aggregate to a 6-h time step; (3) perform various analyses to illustrate differences and similarities between the two mean areal precipitation products; and (4) compare the effects of these inputs on hydrologic simulations produced by one of the hydrologic models used by the NWS. It should be noted here that the 1-h MAPX values were aggregated to 6-h values to provide a direct comparison with the 6-h MAP values. Because of rain gauge reporting characteristics, the current NWSRFS does not allow for the computation of operational MAP values at less than a 6-h time step.

DATA

A total of eight basins were used in the study of precipitation comparisons, with three of these basins being used subsequently in the study of the effects of the precipitation products on the hydrologic simulations. The basins are located mainly on the Oklahoma-Arkansas-Missouri border. Most of the study area stretches north from Fort Smith, Ark. up to Joplin, Mo. Fig. 2 provides a location map of the region and the eight basins. Also shown in Fig. 2 are the rain gauges used to compute operational MAP values. Table 1 provides information regarding the basins.

Operational Gauge Network

Each river forecast center (RFC) within the NWS utilizes data from an operational network of precipitation gauges to

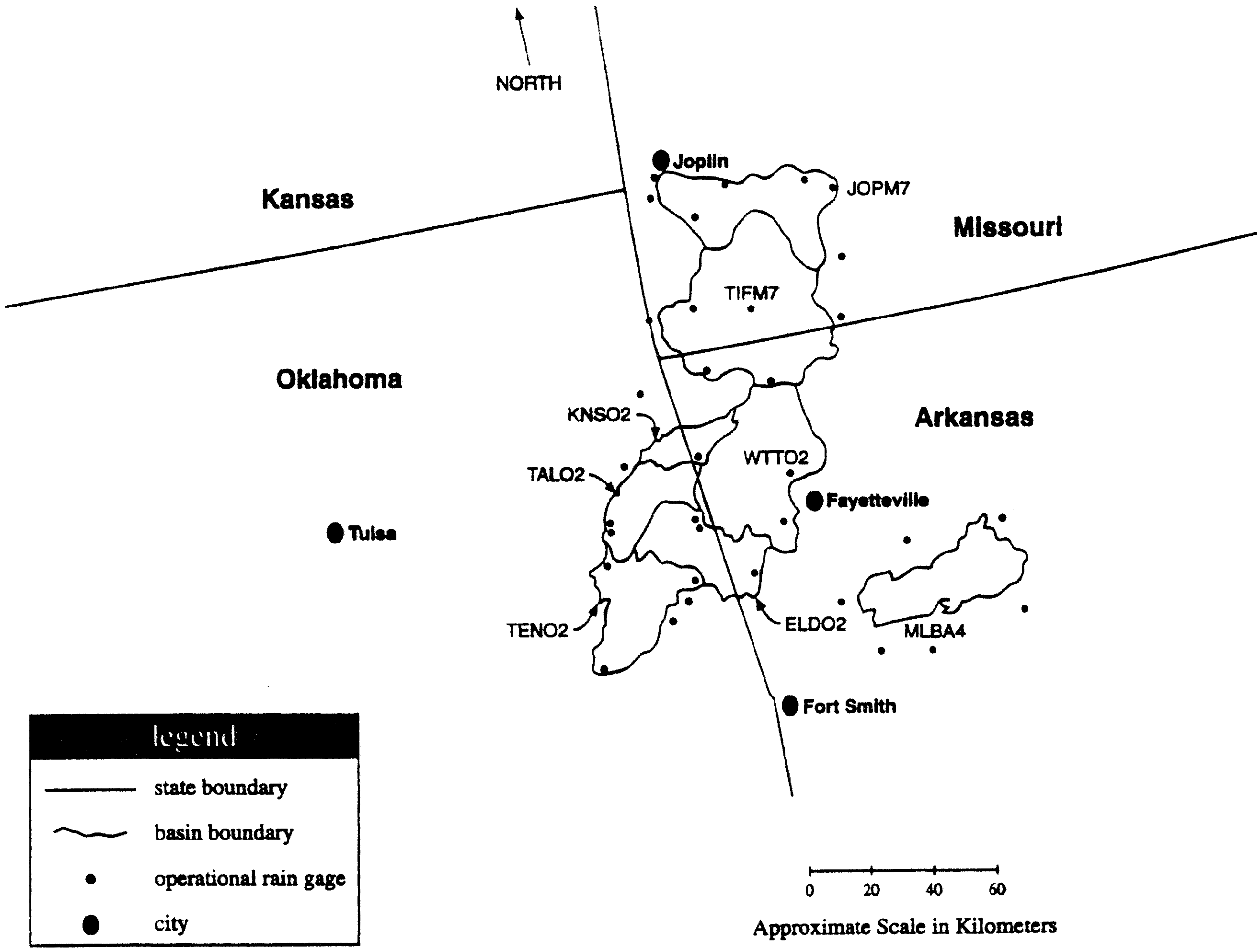

FIG. 2. Location Map of Study Area Showing Test Basins and Rain Gauges Used in Computation of Mean Areal Precipitation Estimates for Operational Forecasting

TABLE 1. Study Basin Descriptions and Relevant Information

Number (1)	Basin name (2)	Latitude/ longitude centroid (3)	Area (km^2) (4)
1	ELDO2: Eldon, Okla.	35.91/94.59	795
2	JOPM7: Joplin, Mo.	36.9/94.17	1,106
3	KNSO2: Kansas, Okla.	36.23/94.58	285
4	MLBA4: Mulberry, Ark.	35.69/93.72	1,103
5	TALO2: Tahlequah, Okla.	36.08/94.78	552
6	TENO2: Tenkiller Ferry Dam, Okla.	35.79/94.88	894
7	TIFM7: Tiff City, Mo.	36.6/94.25	2,259
8	WTTO2: Watts, Okla.	36.12/94.32	1,645

derive MAP values. Details of this procedure can be found in the user's manual for the NWSRFS (National Weather Service 1993). Gauges in the operational network report at a variety of time steps, most commonly 1, 3, 6, and 24 h. In general, rainfall reports from different gauges are accumulated to derive 24-h totals. Missing gauge data are estimated from surrounding gauges using a $1/d^2$ weighting procedure, where d is the distance between the estimator station and the station being estimated. A daily MAP value is computed using one of several weighting options, the most common being a Thiessen polygon method. Daily MAP estimates are then distributed into 6-h periods based on the precipitation values of the gauge closest to the centroid of the basin in each of four quadrants. The MAP values may or may not be exactly reproducible, because of changes in the operational gauge network; however, it is noted that it is considered to be an accurate representation of the precipitation based on the gauge network operating at the time.

Stage III Precipitation

The MAPX products are derived from the gridded hourly NEXRAD stage III precipitation estimates. A brief description of the NEXRAD products is provided here. Additional information can be found in Shedd and Fulton (1993), Seo and Johnson (1995), Finnerty et al. (1997), and Fulton et al. (1997). The NEXRAD product used in this work begins with the raw reflectivity data produced from the radar sites. This raw reflectivity is transformed into precipitation estimates by using a "reflectivity-rainfall" relationship, also known as a "Z-R" relationship. This is known as the stage I product and there are known errors in these precipitation estimates (Smith and Krajewski 1994; Seo et al. 1995; Smith et al. 1996). An attempt to account for these errors results in the processing of the data by utilizing "ground truth" gauge measurements to remove a mean field bias in the radar precipitation estimates; the resulting product is known as a stage II product. Finally, overlapping radar fields are merged in a gridded system known as the NWS Hydrologic Rainfall Analysis Project (HRAP) (Greene and Hudlow (1982) to form a stage III product. The HRAP projection system is a polar stereo graphic projection grid. The grid size varies with location because of the non-equal area projection but is approximately 4 × 4 km^2. The merged data often are referred to as multisensor HRAP precipitation estimates or HRAP precipitation estimates. Essentially, one can think of stage III products as radar-derived distributions that are adjusted to match gauge-recorded precipitation values.

Stage III is the final radar product of an RFC and reflects enhancements and corrections made by a "hydrometeorological analysis and support" (HAS) forecaster at the RFC. Among other tasks, the HAS forecaster checks the stage III products and analyzes the meteorological system that is responsible for the precipitation. The HAS forecaster then may correct or alter the stage III product if it is believed that the radar or gauges used in the stage II product are erroneous. Hourly MAPX values are computed from the stage III data as a spatial average of all the gridded precipitation measurements over a particular basin.

Both the operational MAPs and the MAPXs are considered by the NWS to be very reliable real-time mean areal precipitation estimates over the basin, having been derived from two different approaches.

RESULTS

In these results, we present a variety of data comparing gauge-based MAP and stage III–derived MAPX products. Cumulative amounts for both the MAP and the MAPX estimates are compared, as well as monthly and seasonal totals. Additionally, a number of storms were investigated. The arrival times, storm totals, storm distributions, and return periods were investigated. Because of the large amount of data, the findings are summarized and specific examples are provided to illustrate the general results. In the discussions that follow, we define precipitation bias relative to the rain gauge-derived areal means.

Long-Term Cumulative Sums

The gauge-based MAPs tend to be higher than the radar-based MAPXs. This is true to varying degrees for most of the basins investigated. The basin KNSO2 had cumulative MAPX values that tended to be higher than the MAP values for most of the study period, whereas MLBA4 and TIFM7 had fairly good agreement between MAPX and MAP values over the course of the study period. The remainder of the basins have

TABLE 2. SD and Average Ratio of MAPX Values to MAP Values

Basin name (1)	MAPX/MAP (2)	SD MAPX (3)	SD MAP (4)
ELDO2	0.901	0.1710	0.1567
JOPM7	0.955	0.1430	0.1370
KNSO2	1.153	0.1149	0.1294
MLBA4	1.014	0.1425	0.1556
TALO2	0.941	0.1347	0.1400
TENO2	0.93	0.1490	0.1659
TIFM7	1.012	0.1329	0.1438
WTTO2	0.961	0.1275	0.1332

the MAP values being higher most of the time. This result was found by summing the MAP and MAPX values for each month over the study period and calculating monthly MAPX/MAP ratios. Table 2 presents the average of the 40 monthly ratios for each basin. In some of the basins the ratios are closer than others, but on average, the MAPXs are 5–10% less than the MAPs. Exceptions to this are the basins KNSO2, MLBA4, and TIFM7, for which the MAPX/MAP ratio fluctuated over the period.

Also, overall differences in precipitation amounts were calculated by summing total precipitation over the study period for each year and for the season from May 1 to October 31. This season was selected because of known precipitation estimation errors by the radar in the winter months (Smith et al. 1996). These results are illustrated in Table 3. Note that most of the total bias is achieved in the season from May 1 to October 31, which is not terribly unexpected because most of the precipitation occurs in these months. The overall average bias is 5.4% (MAPX being less than MAP), which is very promising at first glance.

Monthly Precipitation

The conditional average monthly precipitation for the MAPX values is higher than the MAP values. Although the gauge-based MAPs tended to produce higher monthly precipitation (and storm totals), the MAPX time series tended to report fewer increments of precipitation. There were exceptions to this, but in general this tended to be the case. Fig. 3 illustrates the average 6-h mean precipitation (conditioned on the occurrence of precipitation) for the gauge- and NEXRAD-based estimates over the study period for basin ELDO2. Basically, the radar estimates show the storm events occurring in much fewer intervals. Thus, ignoring the underestimation problems of the radar and given cases where the radar and the gauges predicted the same depth of rainfall, the radar estimates

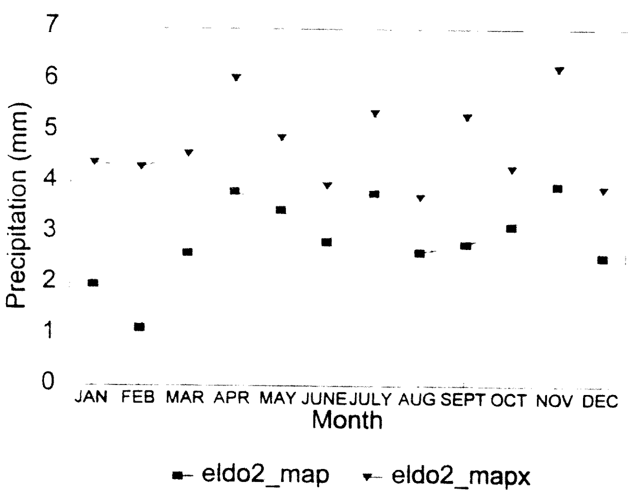

FIG. 3. Conditional 6-h Mean Areal Precipitation Estimates Derived from Radar and Rain Gauges for Basin ELDO2

TABLE 3. Total Study Period Biases and Seasonal Biases and Sum of Total and Seasonal Precipitation (mm)

Statistic (1)	ELDO2 (2)	JOPM7 (3)	KNSO2 (4)	MLBA4 (5)	TALO2 (6)	TENO2 (7)	TIFM7 (8)	WTTO2 (9)
May 1–October 31—MAP	2,931.16	2,994.72	2,186.94	2,484.12	2,694.94	2,961.64	2,847.34	2,410.46
May 1–October 31—MAPX	2,555.24	2,682.24	2,291.08	2,580.64	2,443.48	2,659.38	2,677.16	2,319.02
Seasonal difference (MAPX-MAP)	−375.92	−312.42	+104.14	+96.52	−251.46	−302.26	−170.18	−91.94
Ratio of MAPX/MAP	0.87	0.89	1.05	1.04	0.91	0.90	0.94	0.96
Total precipitation—MAP	4,203.70	3,949.70	3,279.14	3,906.52	3,868.42	4,160.52	3,840.48	3,556.00
Total precipitation—MAPX	3,718.56	3,553.46	3,418.84	3,903.98	3,533.14	3,782.06	3,731.26	3,413.76
Total difference (MAPX-MAP)	−485.14	−396.24	+139.70	−2.54	−335.28	−378.46	−109.22	−142.24
Ratio of MAPX/MAP	0.88	0.90	1.04	1.0	0.91	0.91	0.97	0.96

tended to be more intense and less spread out. Also, it was found that the radar data often showed rainfall as occurring earlier than did the gauge data even at these 6-h increments. Ongoing investigations using 1-h data show this occurs much more frequently at this smaller time step, which is expected (Finnerty and Johnson 1997).

The results presented in Fig. 3 could be the result of two factors. First, the operational gauge network for deriving MAP values is different than the gauge network used in the processing of the NEXRAD estimates to derive MAPX values. Hourly, 3-hourly, 6-hourly, and daily rain gauge reports are used in the MAP algorithm, whereas predominately hourly gauges that report at the top of the hour are used in the processing of NEXRAD data. Also, the strategies used to define a 6-h MAP and MAPX estimates are quite different. As described earlier, in the MAP algorithm a 24-h MAP is derived from the various reports, and then distributed into four 6-h periods based on the temporal distribution of precipitation at four nearby stations. This strategy may tend to spread out the precipitation. If suitable data at nearby stations cannot be found, then the 24-h MAP value is distributed uniformly over four 6-h periods. For example, for basins WTTO2 and ELDO2 between April, 1993 and November, 1996, 71 and 60 cases, respectively, were found in which a uniform distribution was used. In contrast to the MAP algorithm, hourly MAPX values are derived from the stage III data and then aggregated into 6-h MAPX values for use in the hydrologic model.

These differences will have varying effects on hydrologic models. In the case of continuous simulation "bucket" models such as the SAC-SMA, the effects of precipitation biases are cumulative. Current investigations and experience within the NWS show that the SAC-SMA can have difficulty in handling some short-duration, high-intensity events caused by the threshold nature of some of the soil moisture accounting zones.

MAPX/MAP Ratios

No clear trend for the study period could be identified in the MAPX/MAP ratios. In general, MAPX values, as supported by other conclusions in the paper, tend to be lower than MAP values. Examples of this are illustrated in Figs. 4–6, which depict the ratios of MAPX to MAP for the WTTO2, ELDO2, and KNSO2 basins, respectively, for the study period. Also shown in these figures are runoff biases, which will be discussed later. The gap in the plot in September of 1993 in each of the plots is caused by missing data for that month. There may be a slight tendency for the MAPX/MAP ratio to behave less erratically after the first 12 months of the study period.

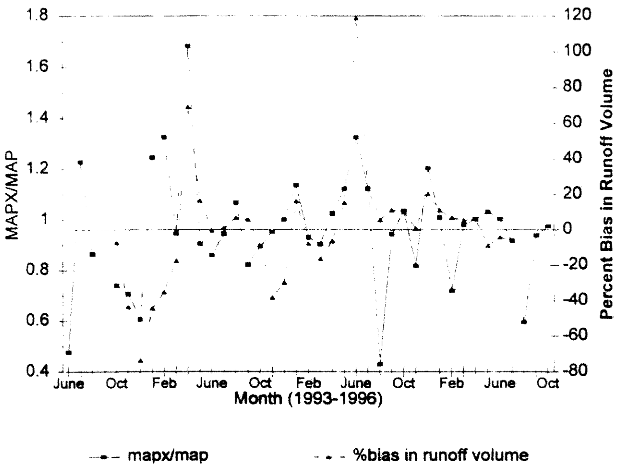

FIG. 4. Ratio of MAPX to MAP and Percent Bias in Runoff Volume for Basin WTTO2

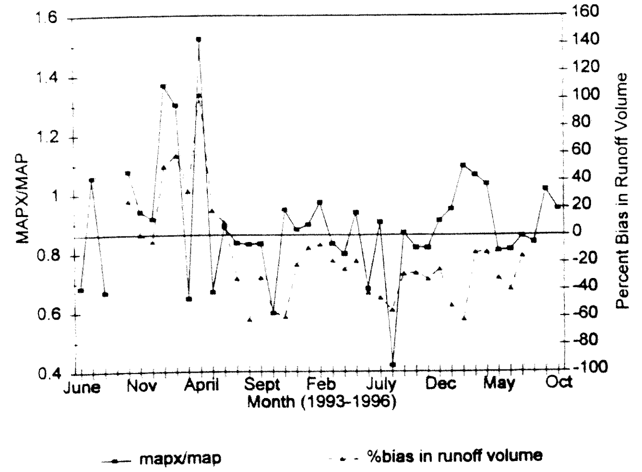

FIG. 5. Ratio of MAPX to MAP and Percent Bias in Runoff Volume for Basin ELDO2

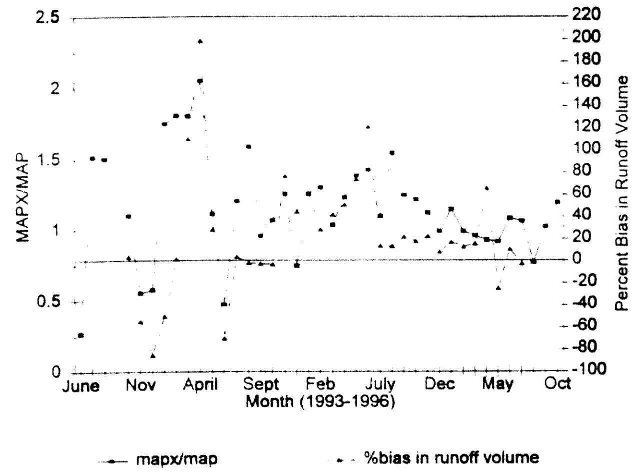

FIG. 6. Ratio of MAPX to MAP and Percent Bias in Runoff Volume for Basin KNSO2

IMPLICATIONS FOR HYDROLOGIC MODELING

To evaluate the hydrologic effects of the MAP versus MAPX differences, streamflow simulations were performed for three of the eight basins using the two precipitation products as input to the SAC-SMA. The basins chosen were WTTO2, ELDO2, and KNSO2, having drainage areas of 1,646, 895, and 285 km^2, respectively.

As mentioned earlier, the SAC-SMA is used widely within the NWS and interested readers are referred to Burnash et al. (1973) and Burnash (1995) for detailed descriptions of the model. In short, the SAC-SMA is a conceptual model consisting of several tension water and free water reservoirs representing the active portions of the soil. Deficits accumulated in the tension water zones must be satisfied before water may move to the free water reservoirs. Fast response surface runoff is generated after upper zone tension and free water storages are full. Moisture is released from the free water reservoirs at different rates and summed with surface runoff to derive a total runoff volume hydrograph. Unit hydrographs are used to transform runoff volumes to discharges.

Parameters for the SAC-SMA for each of the three basins were derived through manual calibration using historical MAP time series derived from NCDC cooperative observer hourly and daily precipitation reports. Observed mean daily flow data from the U.S. Geological Survey were used. Statistics from

TABLE 4. **Calibration Statistics for Three Study Basins**

Basin (1)	WTTO2 (2)	ELDO2 (3)	KNSO2 (4)
Period	1971–1992	1971–1985	1971–1992
Percent bias	4.85	4.78	4.85

the calibration of the three basins in this study appear in Table 4, where the percent runoff bias is computed as follows:

$$\text{bias} = \frac{\sum_{i=1}^{N} (S_i - O_i)}{\sum_{i=1}^{N} O_i} \cdot (100) \quad (1)$$

where bias = percent bias; S = simulated mean daily flow forced with rain gauge data (m^3/2nd day); O = observed mean daily flow (m^3/sec day); and N = number of discharge pairs.

A slight positive bias in runoff volume compared with observed data was realized in the historical calibration of all three basins. Nonetheless, it was felt that the parameter sets were acceptable for the generation of simulated flows using the operational MAP and MAPX time series.

In the current NWSRFS, hydrologic forecasters are provided with techniques that enable them to switch between the use of either the MAPX or the MAP data, depending on which product they think is better. In some RFCs, the switch is made on a seasonal basis, with MAPX being used exclusively in the summer for better detection of convective events. This technique was developed given the assumption that the MAPX and MAP data were similar statistically and that one set of SAC-SMA parameters would be appropriate for both. Given this ability to switch precipitation forcings with the same parameters, it is instructive to evaluate this concept. It is not the intent of this paper to examine the accuracy of simulations derived from each forcing.

Streamflow simulations for the three basins were performed for the period of October 1993–July 1996. Two simulations were produced for each basin: one using the MAPX time series and the other using the MAP values. Model simulations were run using a 6-h time step. It should be emphasized that in each of the three basins, the same SAC-SMA parameters were used for both simulations. Simulated 6-h discharge values were averaged to derive a mean daily flow time series in units of cubic meters per second-day, facilitating the use of existing NWS software for statistical analysis. Table 5 presents the results of these statistical analyses comparing the two simulations. Recall that it is not the intent of this paper to examine explicitly the accuracy of streamflow simulations derived from each forcing.

The bias statistic in Table 5 is computed using the basic form of (1), but modified as shown in (2)

$$\text{bias} = \frac{\sum_{i=1}^{N} (R_i - G_i)}{\sum_{i=1}^{N} G_i} \cdot (100) \quad (2)$$

where bias = percent bias; R = simulated mean daily flow forced with radar data (m^3/sec day); G = simulated mean daily flow forced with rain gauge data (m^3/sec day); and N = number of discharge pairs.

The total bias is computed as the difference of the average monthly simulated and observed flows divided by the average monthly observed flow. It can be seen from Table 5 that the simulations produced from the two input forcings are significantly different on a seasonal basis.

In addition to the MAPX/MAP ratio, Fig. 4 also presents the runoff bias for each month in the simulation period for WTTO2. The plots in this figure reveal that in general, the runoff volume bias corresponds to the MAPX/MAP ratio. However, it can be noticed that the runoff bias lags the MAPX/MAP ratio for the first few months of the simulation period. For example, Fig. 4 shows MAPX/MAP ratios less than 1.0 for October, November, and December of 1993, followed by 2 months in which the MAPX/MAP ratio is greater than 1.0. In April 1994, the MAPX/MAP ratio climbs to 1.7. Examination of Fig. 4 shows that although the MAPX/MAP ratio is greater than 1.0 for January and February 1994, a corresponding positive bias in runoff volumes does not occur until April 1994.

This delayed response of the runoff bias is logical considering the structure of the SAC-SMA. In those months in which MAPX values are less than MAP, larger soil moisture deficits are created in the radar-forced model compared with the gauge-forced model. Even though in subsequent months the MAPX/MAP ratio is greater than 1.0, the larger deficits in the radar-forced model require more precipitation to be satisfied before runoff can be produced.

Fig. 4 shows that a large runoff volume bias was generated in June 1995. Examination of the MAPX and MAP time series reveals that this bias is the result of a single precipitation event beginning on June 10. As shown in Table 6, NEXRAD measured over 27 mm more precipitation than did the rain gauge network. Also, the most intense 6-h period of rainfall in the MAPX time series occurred one time step earlier than the most intense period of gauge-recorded rainfall.

TABLE 5. Percent and Absolute Biases in Monthly Runoff Volumes Generated Using MAP and MAPX Time Series (Period Is October 1993–July 1996)

	BASIN					
	WTTO2		ELDO2		KNSO2	
Month (1)	% (2)	mm (3)	% (4)	mm (5)	% (6)	mm (7)
October	−4.2	−0.5	3.9	0.7	6.1	0.4
November	−37.3	−7.2	−38.5	−21.5	−5.0	−0.7
December	−49.6	−12.7	−20.9	−7.0	−50.4	−15.0
January	4.9	1.2	−16.1	−8.1	−34.4	6.8
February	−17.6	−2.2	7.9	1.6	−16.3	1.3
March	−16.3	−5.9	−32.6	−24.5	77.6	15.8
April	21.0	8.0	1.1	0.6	102.5	34.8
May	10.0	4.5	−21.7	−13.4	38.8	14.9
June	70.3	13.8	−43.7	−13.8	41.8	13.3
July	9.1	1.0	−44.7	−8.2	6.9	0.6
August	11.6	1.0	−65.2	−13.1	6.2	0.5
September	8.8	0.6	−36.5	−2.1	9.8	0.6
Total	0.5	1.8	−23.0	−108.8	33.0	73.1

TABLE 6. MAPX and MAP Values for June 10, 1995, Event in WTTO2

Date (1)	Time (2)	MAP value (mm) (3)	MAPX value (mm) (4)
June 8	24	8.00	8.61
June 9	6	3.12	1.60
June 9	12	2.62	8.71
June 9	18	0.0	0.03
June 9	24	8.26	5.38
June 10	6	0.02	0.0
June 10	12	0.10	7.26
June 10	18	6.78	33.88
June 10	24	21.18	14.12
June 11	6	0.0	0.0
June 11	12	1.65	0.15
June 11	18	3.33	2.79
Total		55.13	82.53

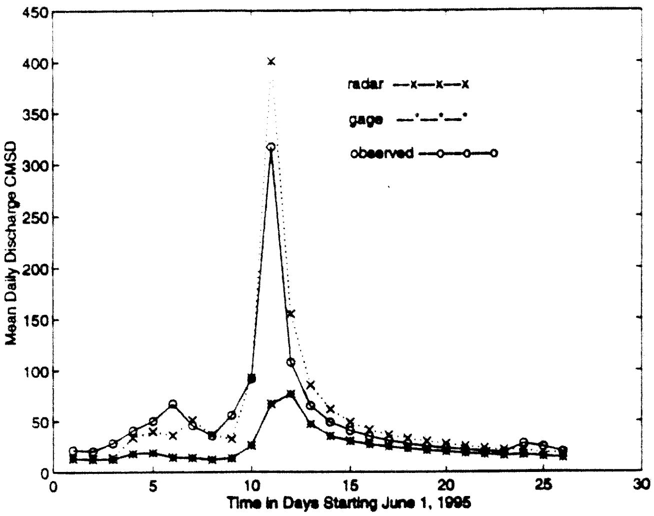

FIG. 7. Simulate Hydrographs for June 13, 1995, Event in Basin WTTO2: Radar versus Gauge Forcing

The plot of the observed and simulated discharge hydrographs in Fig. 7 reveals that the MAPX-forced simulation produced much more runoff than the MAP-forced simulation. Although overpredicting the observed discharge, the MAPX-forced simulation is far better than the MAP-forced case. Examination of the radar rainfall patterns for this event reveal that some parts of the basin received little precipitation compared with others, implying that the gauge network may have misrepresented the event in a similar fashion to the case discussed by Barge et al. (1979). Examination of the initial conditions in each simulation revealed no major differences, so that the simulated hydrographs in Fig. 7 are largely the result of the differences in event MAPX and MAP values.

Results very similar to those in Fig. 7 also were achieved for an event in January 1995 in basin WTTO2. Initially, it was not clear whether the good fit produced using radar data was caused by oversimulation of the precipitation because of bright band contamination, or whether the radar simply captured the precipitation better than the gauge network. Bright band contamination is caused when a radar beam passes through the zero-degree isotherm layer in the atmosphere (Battan 1973; Collier et al. 1975; and Hopper et al. 1991). Precipitation above this line is more in the form of frozen particles. As this frozen precipitation passes through the zero-degree isotherm, it begins to melt, producing particles of water-coated ice droplets. These droplets are capable of reflecting high levels of energy, thus producing stronger radar echos that appear as areas of high rainfall. Subsequent analysis of the stage III data by ABRFC personnel revealed that there was no bright band contamination for this event, indicating that the better simulation was the result of a better estimate of the precipitation.

Behavior similar to Fig. 4 appears in Fig. 5 for ELDO2. In general, the monthly runoff biases correspond in time to the MAPX/MAP ratio. In April 1994 a large bias can be identified. In this case, the MAPX values for an event on April 5 are almost double the MAP values. As a result, the MAPX-forced simulation exhibited a strong runoff response (not shown here), whereas the MAP-forced simulation showed almost no hydrograph rise at all. Observed streamflow records reveal no significant runoff response for this rainfall event, indicating that the radar greatly overpredicted the amount of precipitation for this event. From April 1994 to the end of the simulation period, Fig. 5 shows quite a strong negative bias in runoff volumes. This result is understandable in that the overall MAPX/MAP ratio of 0.88 indicates less rain detected by the radar.

Fig. 6 shows the same erratic behavior of the runoff volume ratio for basin KNSO2 that was seen for basins ELDO2 and WTTO2. A large bias can be seen for the month of April 1994, largely caused by the event on April 9–11, in which the radar recorded 81.3 mm of rainfall and the gauge network recorded 35.6 mm. Although not shown here, there is no observed discharge data for this event, so it is not possible to judge the simulations forced using the two data sources. After this event, Fig. 6 shows a general positive runoff bias, which is reasonable considering that the average MAPX/MAP ratio is 1.15. The large bias in June of 1995 is caused by a single event in which the radar greatly overestimated the precipitation compared with the gauge network estimate.

Although the purpose of the hydrologic modeling was to compare MAPX and MAP network-forced streamflow simulations using rain gauge-calibrated model parameters, it was nonetheless interesting to also compare visually both simulations to observed streamflow records for storm events. In some cases, the MAPX-forced simulations performed better than the gauge-forced simulations. However, in others, either the MAP-forced simulations were better or the MAPX-forcing produced hydrograph responses that were not seen in the observed streamflow records. More comprehensive testing should address the issue of the accuracy of streamflow simulations generated by MAPX and MAP data.

CONCLUSIONS

Although much of this work continues, some conclusions can be made at the present time. With regard to overall performance, the NEXRAD system produces viable mean areal precipitation estimates. A problem of inconsistency is identified; however, the level to which these inconsistencies will affect hydrologic and climatologic models has yet to be determined.

Compared with gauge-only estimates of mean areal precipitation, the radar produces slightly lower values. This may affect climate and hydrologic models that rely on this data for calibration. We have shown that in the southern plains region, which has a relatively dense network of rain gauges and multiple overlapping radars, the radar estimates are approximately 5–10% lower than the gauge estimates, after correction by NWS HAS forecasters. If historical gauge networks are used to calibrate models, then use of the radar products may affect the model outcomes. The bias appears to be decreasing (at least in stage III products), perhaps because forecasters learn to better utilize and correct the radar estimates.

We have compared two operational products of the NWS Tulsa River Forecast Center. Some of these products, particularly the NEXRAD precipitation products are available to the public. It is hoped that this work will provide some guidance for proper usage. Statistical differences in the MAPX and MAP time series resulted in significant impacts on streamflow simulations. Large biases can result in both runoff volumes and peak flows for certain events.

As one might expect, overall biases in runoff volumes correspond to biases in input forcing. For example, the long-term MAPX/MAP ratio for basins WTTO2 and ELDO2 are 0.961 and 0.901, respectively, which lead to percent biases in the runoff volumes of 0.5 and −23.0. A percent runoff bias of 33.0 for basin KNSO2 resulted from the MAPX/MAP ratio of 1.153. Even larger monthly biases were seen in the simulations of the three basins. Inconsistent behavior was noted when storm events were examined. At times, the radar-derived mean areal estimates of precipitation led to better streamflow simulations. At other times, the radar-derived estimate led to simulated hydrograph responses that were not evident in the observed discharge records.

Given the runoff biases, it is important that efforts be made to calibrate the hydrologic model parameters to the anticipated type of forcing. In the examples presented, the SAC-SMA was calibrated for three basins using multiyear MAP time series derived from an historical gauge network. Use of these parameters may lead to suboptimal simulations when forced with radar precipitation measurements or data from the operational gauge network. It has long been assumed in the NWS that the MAP time series used for calibration are unbiased compared with MAP time series derived from the operational gauge network. Further research should be performed to include a comparison of MAPs from the calibration network with the operational MAPX and MAP values. Moreover, testing should be performed to evaluate the accuracy of hydrologic simulations forced by MAP and MAPX data. In such tests, SAC-SMA parameters should be calibrated to each forcing and subsequent streamflow simulations compared with observed data.

ACKNOWLEDGMENTS

Dr. Lee Larson, Chief of the Hydrologic Research Lab, deserves credit for facilitating this research. The writers would like to thank Robert Motl for his programming assistance in deriving the time series data files. Comments and assistance from Bill Lawrence and others at the NWS River Forecast Center in Tulsa, Okla. are appreciated. Dr. D. J. Seo provided many comments on the interpretation of results. The comments of two anonymous reviewers are greatly appreciated.

APPENDIX. REFERENCES

Barge, B. L., Humphries, R. G., Mah, S. J., and Kuhnke, W. K. (1979). "Rainfall measurements by weather radar: Applications to hydrology." *Water Resour. Res.*, 15(6), 1380–1386.

Battan, L. J. (1973). *Radar observation of the atmosphere*. University of Chicago Press, Chicago.

Borga, M., Da Ros, D., Fattorelli, S., and Vizzaccaro, A. (1995). "Influence of various weather radar correction procedures on mean areal rainfall estimation and rainfall-runoff simulation." *Proc., 3rd Int. Symp. on Hydro. Applications of Weather Radar*, ABRH, International Association of Hydraulic Research, Sao Paulo, Brazil, 146–157.

Burnash, R. J. C. (1995). "The NWS river forecast system—Catchment modeling." *Comp. models of watershed hydrology*, V. P. Singh, ed., Water Resources Publications, Littleton, Colo., Chapter 10, 311–366.

Burnash, R. J. C., Ferral, R. L., and McGuire, R. A. (1973). "A generalized streamflow simulation system—Conceptual modeling for digital computers." U.S. Department of Commerce, National Weather Service and State of California, Department of Water Resources, Sacramento, Calif., Silver Spring, Md.

Collier, C. G., Harrold, T. W., and Nicholass, C. A. (1975). "A comparison of areal rainfall as measured by a raingauge-calibrated radar system and raingauge networks of various densities." *Proc., 16th Meteorology Conf.*, American Meteorological Society, Boston, 467–472.

Finnerty, B. D., and Johnson, D. (1997). "Comparison of National Weather Service operational mean areal precipitation estimates derived from NEXRAD radar vs. raingage networks." *Presented at the IAHR XXVII Congr.*, International Association of Hydraulic Research, Delft, The Netherlands.

Finnerty, B. D., Smith, M. B., Koren, V., Seo, D. J., and Moglen, G. (1997). "Space-time scale sensitivity of the Sacramento model to radar-gage precipitation inputs." *J. Hydrol.*, Amsterdam, 203, 21–38.

Fulton, R. A., Briedenbach, J. P., Seo, D. J., Miller, D. A., and O'Bannon, T. (1998). "The WSR-88D rainfall algorithm." *Weather and Forecasting*, 13(2), 377–379.

Goodhew, R., and Mylne, M. (1992). "Measurement of areal rainfall by an operational radar at medium range." *Paper No. H2, Proc., 2nd Int. Symp. on Hydro. Applications of Weather Radar*, University of Hannover, Hannover, Germany.

Greene, D. R., and Hudlow, M. D. (1982). "Hydrometeorological grid mapping procedures." *AWRA Int. Symp. on Hydrometeorology*, American Water Resources Association, Bethesda, Md.

Hopper, S. E., Illingworth, A. J., and Caylor, I. J. (1991). "Bright-band errors in rainfall measurement: Identification and correction using linearly polarized radar returns." *Hydrological applications of weather radar*, I. C. Cluckie and C. G. Collier, eds., Ellis Horwood Series in Environmental Management, Science and Technology, Chichester, West Sussex, England, 240–249.

Hudlow, D. D. (1988). "Technological developments in real-time operational hydrologic forecasting in the United States." *J. Hydro.*, Amsterdam, 102, 69–92.

Klazura, G. E., and Imy, D. A. (1993). "A description of the initial set of analysis products available from the NEXRAD WSR-88D system." *Bull. Am. Meteorological Soc.*, Boston, 74(July), 1293–1311.

National Weather Service. (1993). *OFS MAP preprocessor function*. National Weather Service River Forecast System User's Manual, National Weather Service, Silver Spring, Md.

Seo, D. J., Fulton, R., Breidenbach, J. P., Miller, D., and Friend, E. (1995). "Final report for October 1, 1993 to October 31, 1994." Interagency Memorandum of Understanding among the NEXRAD Program, WSR-88D Operational Support Facility, and the National Weather Service Office of Hydrology, Hydrologic Research Laboratory, Silver Spring, Md.

Seo, D. J., and Johnson, E. R. (1995). "The WSR-88D precipitation processing subsystem—An overview and a performance evaluation." *Proc., 3rd Int. Symp. on Hydro. Applications of Weather Radar*, I.A.H.R., Delft, The Netherlands, 222–231.

Shedd, R. C., and Fulton, R. A. (1993). "WSR-88D precipitation processing and its use in the National Weather Service hydrologic forecasting." *Proc. of ASCE Int. Symp. on Engrg. Hydr.*, ASCE, Reston, Va., 25–30.

Smith, J. A., and Krajewski, W. (1994). "Final report—Estimation of parameters for the NEXRAD rainfall algorithms." Submitted to NOAA National Weather Service, Office of Hydrology, Hydrologic Research Laboratory.

Smith, J. A., Seo, D. J., Baeck, M. L., and Hudlow, M. (1996). "An intercomparison study of NEXRAD precipitation estimates." *Water Resour. Res.*, 32(7), 2035–2045.

Smith, P. L., Cain, D. E., and Dennis, A. S. (1975). "Derivation of an R-Z relationship by computer optimization and its use in measuring daily areal rainfall." *Proc., 16th Radar Meteorology Conf.*, American Meteorological Society, Boston.